Spatial and biological oceanographic insights into the massive fish-killing bloom of the haptophyte *Chrysochromulina leadbeateri* in northern Norway

Uwe John [a,b,*], Luka Šupraha [c], Sandra Gran-Stadniczeñko [c], Carina Bunse [b,d], Allan Cembella [a], Wenche Eikrem [c], Jan Janouškovec [c], Kerstin Klemm [a], Nancy Kühne [a], Lars Naustvoll [e], Daniela Voss [d], Sylke Wohlrab [a,b], Bente Edvardsen [c]

[a] *Alfred Wegener Institute, Helmholtz Centre for Polar and Marine Research, Am Handelshafen 12, 27570 Bremerhaven, Germany*
[b] *Helmholtz Institute for Functional Marine Biodiversity at the University of Oldenburg (HIFMB), Ammerländer Heerstraße 231, 26129 Oldenburg, Germany*
[c] *Section for Aquatic Biology and Toxicology, Department of Biosciences, University of Oslo, P.O. Box 1066 Blindern, 0316 Oslo, Norway*
[d] *ICBM: Institute for Chemistry and Biology of the Marine Environment, University of Oldenburg, Carl-von-Ossietzky-Straße 9-11, 26129 Oldenburg, Germany*
[e] *Institute of Marine Research, P.O box 1871 Nordnes, NO-5817 Bergen, Norway*

ARTICLE INFO

ABSTRACT

A bloom of the fish-killing haptophyte *Chrysochromulina leadbeateri* in northern Norway during May and June 2019 was the most harmful algal event ever recorded in the region, causing massive mortalities of farmed salmon. Accordingly, oceanographic and biodiversity aspects of the bloom were studied in unprecedented detail, based on metabarcoding and physico-chemical and biotic factors related with the dynamics and distribution of the bloom. Light- and electron-microscopical observations of nanoplankton samples from diverse locations confirmed that *C. leadbeateri* was dominant in the bloom and the primary cause of associated fish mortalities. Cell counts by light microscopy and flow cytometry were obtained throughout the regional bloom within and adjacent to five fjord systems. Metabarcoding sequences of the V4 region of the 18S rRNA gene from field material collected during the bloom and a cultured isolate from offshore of Tromsøy island confirmed the species identification. Sequences from three genetic markers (18S, 28S rRNA gene and ITS region) verified the close if not identical genetic similarity to *C. leadbeateri* from a previous massive fish-killing bloom in 1991 in northern Norway. The distribution and cell abundance of *C. leadbeateri* and related *Chrysochromulina* species in the recent incident were tracked by integrating observations from metabarcoding sequences of the V4 region of the 18S rRNA gene. Metabarcoding revealed at least 14 distinct *Chrysochromulina* variants, including putative cryptic species. *C. leadbeateri* was by far the most abundant of these species, but with high intraspecific genetic variability. Highest cell abundance of up to 2.7×10^7 cells L^{-1} of *C. leadbeateri* was found in Balsfjorden; the high cell densities were associated with stratification near the pycnocline (at ca. 12 m depth) within the fjord. The cell abundance of *C. leadbeateri* showed positive correlations with temperature, negative correlation with salinity, and a slightly positive correlation with ambient phosphate and nitrate concentrations. The spatio-temporal succession of the *C. leadbeateri* bloom suggests independent initiation from existing pre-bloom populations in local zones, perhaps sustained and supplemented over time by northeastward advection of the bloom from the fjords.

1. Introduction

Harmful Algal Blooms (HABs) are a recurring phenomenon in northern Europe, particularly along the coasts of the Baltic Sea, Kattegat-Skagerrak, North Sea, Norwegian Sea and the adjacent Barents Sea (Karlson et al., 2021). These HABs have at times caused major losses to the aquaculture and fishing industries, posed a risk to human health from toxic seafood consumption, disrupted local ecosystem functioning and chronically affected socioeconomic interests in various ways (reviewed in Bresnan et al., 2021). Operationally, and in terms of monitoring strategies and event reporting, HABs and their consequences in northern Europe can be roughly subdivided into two categories

---

(Harmful Algae Event Database, HAEDAT http://haedat.iode.org, 2021): i) high cell density blooms often covering large coastal areas that cause mortalities of fish and other marine fauna and/or damage to ecosystem function, e.g. disruption of food webs or oxygen depletion, or loss of recreational opportunities due to biofouling of beaches and coastal waters; and ii) those causing contamination of seafood by phycotoxin accumulation, especially in shellfish, even at comparatively low algal cell densities. Fish-killing HABs are functionally distinct from those responsible for shellfish toxicity (Hallegraeff et al., 2021). Such fish-killing blooms may cause mortalities and morbidities by a variety of mechanisms, including mechanical effects on gills (e.g. via spines), blockage and gill membrane damage by physical contact and/or mucus production by dense bloom-forming microalgae, direct ichthyotoxicity by potent toxins, (Andersen et al., 2015; Mardones et al., 2019), or indirect effects of oxygen depletion following bloom senescence.

Major fish killing events in northern Europe are highly sporadic and unpredictable, and the socioeconomic impacts are linked to expansion of fish aquaculture activities, especially in Norway, Faroe Islands, west Scotland and the Shetland Islands, the coast of Ireland and the northern Atlantic coast of France (Bresnan et al., 2021). In most cases in Scandinavia, these fish-killing events have been directly linked to blooms of marine haptophytes, particularly members of the genera *Prymnesium* and *Chrysochromulina*. The first recorded major haptophyte-linked HAB event in Scandinavia occurred in May-June 1988, when *Prymnesium polylepis* (formerly *Chrysochromulina polylepis*) formed a large toxic bloom in the Kattegat, Skagerrak, and eastern North Sea (Dahl et al., 1989; Edvardsen and Paasche, 1998; Skjoldal and Dundas, 1991). The bloom disrupted the entire ecosystem, and severely impacted plankton communities (Nielsen et al., 1990), benthic flora and fauna, and killed both wild and farmed fish (Gjøsæter et al., 2000).

The Norwegian salmon industry in particular has suffered periodic significant losses caused by massive algal blooms over past few decades. In the period 1989–1995, *P. parvum* formed blooms causing annual mortalities at salmon farms in Ryfylke in western Norway, but these mortality events subsided when the fish farms were relocated to other areas or cages were submerged to 10 m during the bloom peak (Johnsen et al., 2010). *Chrysochromulina leadbeateri* was first reported as the cause of mortalities at fish farms in the Lofoten archipelago and Vestfjorden in northern Norway in late May 1991 (Rey, 1991). Three decades later, this species again formed a massive fish-killing bloom in early May – June in Vestfjorden in the Lofoten area (Vesterålen) and further north near Tromsø, killing at least 14,500 t of farmed salmon in Nordland, Troms and Finnmark counties in northern Norway (Samdal and Edvardsen, 2020). Direct and indirect gross economic losses are estimated between 2.3–2.9 billion (NOK) (ca. 300 million $US) (Marthinussen et al., 2020). This is the largest fish kill caused by a HAB event ever recorded in Norway and at least in economic terms also in northern Europe.

About 20 species of *Prymnesium* and nearly 50 of *Chrysochromulina* belonging to the order Prymnesiales have been formally described among the haptophytes (Guiry and Guiry, 2021), of which approximately 40 are reported from Scandinavian coastal waters (Edvardsen et al., 2016; Norwegian Biodiversity information center https://www.biodiversity.no). All haptophytes are assumed to be mixotrophic to some degree, but phagotrophy has been conclusively demonstrated in only a few species (Avrahami and Frada, 2020). Mixotrophic haptophytes are capable of prey capture and ingestion of organic particulates, typically bacteria and small eukaryotes, facilitated by their typically sticky haptonema.

Some haptophytes form high biomass blooms, including a few implicated in HAB events, whereas others are recorded only at low cell densities between 10^3 and 10^5 cells L^{-1} (Thomsen et al., 1994). In Scandinavian waters, haptophyte blooms are particularly common in fjords and estuaries or near the coast, such as in the Skagerrak. Members of Prymnesiales typically form high magnitude blooms ($>1 \times 10^6$ cells L^{-1}) during warm and sunny conditions, and in stratified water even with low inorganic nutrient concentrations (N, P) in the upper mixed layer

(Lekve et al., 2006). This has led to general hypotheses concerning the key abiotic ecological factors favoring haptophyte blooms – high N:P ratios, high organic nutrients, coupled with low salinity, reduced vertical mixing and high solar irradiance, i.e., a stratified regime (Edvardsen and Paasche, 1998; Lekve et al., 2006). Nevertheless, models to predict selective advantages among the key haptophyte HAB species, such as *C. leadbeateri*, *P. polylepis* and *P. parvum* responsible for fish kills in the Norwegian Sea and adjacent waters are lacking.

Reliable oceanographic, taxonomic and species diversity data linked to *in situ* development of HABs of fish-killing haptophytes and resulting fish kills are rarely available. This is largely because such blooms are difficult to anticipate from routine phytoplankton species monitoring and associated harmful events are infrequent in northern Europe. Hence, it is challenging to develop a field monitoring strategy linked to fixed oceanographic campaigns on an appropriate spatial-temporal scale to describe bloom dynamics and biogeographical distribution.

An oceanographic expedition already underway to study biological oceanographic processes in fjord systems of northern Norway with a focus on HAB species provided a unique opportunity to explore in situ the massive devastating bloom of *C. leadbeateri*. Metabarcoding sequences and morphological characteristics of *Chrysochromulina* variants from field populations were compared with strains isolated from the blooms. Morphological and molecular genetic analysis of samples of the nanoplankton communities were considered in the context of the biological, chemical, and physical oceanographic conditions and advective processes in the region during the bloom. This study provides a partial template for future incorporation into conceptual models of haptophyte dynamics linked to major fish kills along the Norwegian coast.

2. Material and methods

2.1. Oceanographic and plankton sampling procedures

2.1.1. Oceanographic data

Oceanographic data on physical and biophysical parameters were collected during the HE533 expedition aboard *RV Heincke* from Vesterålen to Tanafjorden in northern Norway between 20th May and 6th June 2019. Six transects along the long axis of six fjord systems were sampled at 28 stations. (Fig. 1). Oceanographic and biooptical data were acquired with a SBE911+ CTD (Sea-Bird Electronics, USA), equipped with additional sensors for turbidity, oxygen, and in vivo fluorescence. Before plankton sampling, the chlorophyll fluorescence profile and depth of the deep chlorophyll maximum layer (DCM) were identified to guide sampling at each station. The CTD data are available in Pangaea® (John and Wisotzki 2019, https://doi.org/10.1594/PANGAEA.903511), and detailed post-processing of the complete CTD workflow is given within the HE533 Data Processing Report (Rohardt, 2019, hdl:10,013/epic.d9f486d9–4d03–4f9a-99bb-8fb3a44578e0). For nutrients and DCM values also see supplementary Table 1.

2.1.2. Plankton sampling and archiving

At each station, 20 L of seawater was collected at three discrete depths (3 m, 40 m and the DCM varying between 8 and 28 m) with Niskin bottles deployed on a rosette sampler. Samples for inorganic nutrients (N, P, Si) and identification and quantitative analysis by light microscopy and flow cytometry were selected from the three discrete depths, whereas 21 L seawater were pooled from the three depths for metabarcoding. Pooled plankton-containing seawater was sieved by sequential gravity filtration over 200 μm and 20 μm mesh-size Nitex sieves. This was followed by sequential in-line filtrations through 3 and 0.2 μm polycarbonate membranes (147 mm diameter, Millipore, Darmstadt, Germany) with a peristaltic pump for a maximum 30 min. These filtrations yielded three operationally defined size-fractions: microplankton (20 - 200 μm), nanoplankton (3 - 20 μm), and picoplankton (0.2 - 3 μm). Filters were immersed in warm (approximately 60 °C) lysis buffer from the nucleotide extraction kits described below in
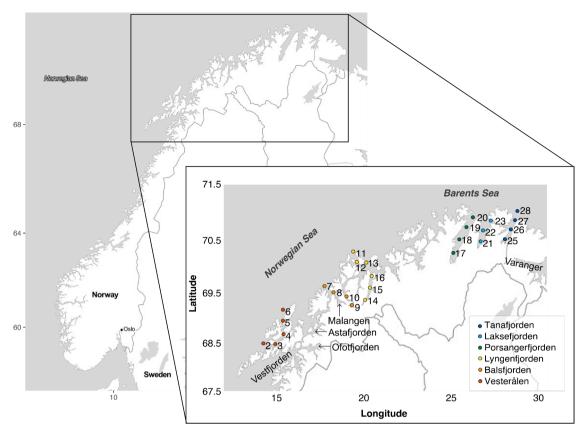
Fig. 1. Sampling area and stations investigated aboard *RV Heincke* cruise HE533. Transects along the northern Norwegian coast included Vesterålen (St 2–6), Balsfjorden (St 7–10), Lyngenfjorden (St 11–16), Porsangerfjorden (St 17–20), Laksefjorden (St 21–23), and Tanafjorden (St 25–28).

2 mL cryotubes, then fast-frozen and kept at −80 °C until further processing.

2.2. Light microscopic counts and identification of C. leadbeateri

Water samples for on-board quantitative analysis of protist communities were collected from Niskin bottle casts at all stations. Seawater samples (50 mL) from the surface layer (3 m) and from the DCM were fixed with Lugol's iodine solution (1% final concentration) and left to sediment for 24 h in a 50 mL Falcon tube. After sedimentation, the top 45 mL were sucked away by Pasteur pipette with tubing attached to a peristaltic pump. A sub-sample (0.1 mL) of 10x concentrate was transferred to a Palmer-Maloney counting chamber (PhycoTech Inc., St. Joseph, MI, USA) for on board analysis under the light microscope (Zeiss AxioPlus, Jena, Germany). All protist cells were identified to lowest reliable taxonomic level and counted for the entire chamber. Cell densities from original seawater samples (cells L^{-1}) were calculated from the specific conversion factor for Palmer-Maloney chambers (0.1 mL) and the initial 10x concentration of sedimented samples. *Chrysochromulina leadbeateri* cells were identified with certainty by phase-contrast microscopy (400x magnification) based on their characteristic size, rounded shape, the presence of two chloroplasts, two long flagella and a coiling haptonema slightly longer than the flagella. The standard taxonomic reference for identifying *Chrysochromulina* species along the Norwegian coast is "Phytoplankton of Norwegian Coastal Waters" by Throndsen, Hasle and Tangen (2007), as well a publication by Eikrem and Throndsen (1998). Throndsen, Hasle and Tangen (2007) was also used as a taxonomic reference while counting phytoplankton samples during the cruise.

2.3. Flow cytometry

Flow cytometry analysis was conducted on board within 2 h after Niskin bottle water samples were retrieved from 3 m depth and DCM (8–28 m) surface layers. The size distribution and cell counts for live autofluorescent phytoplankton were determined in duplicate 500 μL water samples with an Accuri C6 flow cytometer (BD Biosciences, Erembodegem, Belgium) in the fast mode (500 μL in 7.38 min), with threshold 900 in FL3 channel. Internal fluidics were maintained with MilliQ® water with laser calibration confirmed with Spherotech 6-Peak and 8-Peak Validation Beads from BD Biosciences. The data were analyzed with BD Accuri C6 C-Flow software (Version 1.0.264.21). Cytograms of red fluorescence (FL3, >670 nm), orange fluorescence (FL2, 585 nm) and forward- and side-scatter (FSC and SSC, respectively) upon excitation by blue laser (488 nm) were plotted to manually gate plankton cell abundances, as proposed in Gasol and Morán (2015) (and shown in Suppl. Fig. 1). Picoeukaryotes (Pk) were derived from the FL3/FL2 cytogram as a group of small cells with low FL2- and FL3-signals; cryptophytes (Nk1) were defined as nanoeukaryotes with FL2-signal; other small nanoeukaryotes (Nk2) exhibited medium FL3-signal, but no FL2-signal; and large nanoeukaryotes (Nk3) were distinguished by high FL3-signal, but no FL2-signal. The FL2/FSC (forward scatter) cytogram revealed a cyanobacterial cluster (Cyano) with intermediate FL2-signal, but low FSC-signal, indicating small cells.

2.4. Metabarcoding of eukaryotic and prokaryotic rRNA genes

DNA was extracted with the NucleoSpin® Soil kit (Macherey-Nagel, Düren Germany) following the manufacturer's protocol. A bead beater (MagNA Lyser, Roche, Basel, Switzerland) was applied (2 × 30 s bursts) with glass beads to break up the cells in lysis buffer. The variable V4 region of the 18S rRNA eukaryote gene was amplified with the primer

set of Piredda et al. (2017) with overhanging Illumina adapters. The prokaryote community composition was determined based on the V4 and V5 hypervariable regions of the 16S rRNA gene amplified with the forward primer MS_V4_515F_N (Apprill et al., 2015) and reverse primer MS_V4_806R_1 (Parada et al., 2016).

PCR amplification and library construction were performed as described in the Illumina 16S metagenomic sequencing library preparation (https://support.illumina.com/downloads/16s_metagenomic_sequencing_library_preparation.html, doc.no:15044223B), with slight modifications (e.g. the use of different primers) for 18S rRNA gene amplicon preparation. Briefly, the 25 µL PCR reaction mix consisted of 2.5 µL genomic DNA (5–10 ng), 5 µL 1 µM forward primer, 5 µL 1 µM reverse primer, and 12.5 µL 2x KAPA HiFi HotStart ReadyMix (KAPA-Biosystems, Boston, USA). The PCR-program included an initial denaturation at 95 °C for 3 min, followed by 25 cycles at 95 °C for 30 s, annealing at 55 °C for 30 s, extension at 72 °C for 30 s, and a final extension at 72 °C for 5 min. PCR reactions were cleaned with CleanNGS beads (CleanNA, Waddinxveen, Netherlands) and pooled in equimolar concentrations. The amplicon libraries were sequenced using the MiSeq Reagent Kit v3 (600-cycle) MS-102–3003 in a MiSeq Sequencer (Illumina, San Diego, US).

2.5. Bioinformatic processing

Primers and spurious sequences were trimmed with CUTADAPT v.3.5 (Martin, 2011). The DADA2 pipeline (Callahan et al., 2016) was used to quality filter, trim, remove chimeras and denoise the reads into amplicon sequence variants (ASVs). The taxonomic assignment was done with reference to the Protist Ribosomal Reference Database (PR2 v.4.12, (Guillou et al., 2013, https://github.com/vaulot/pr2database). This assignment yielded a total of 4231 nanoplankton protist ASVs.

A total of 230 ASVs from the metabarcoding dataset were identified as belonging to haptophytes during the taxonomic assignment step of bioinformatic processing. To identify ASVs assigned to genus *Chrysochromulina*, the haptophyte ASVs were added to the curated and updated 18S rRNA gene haptophyte reference alignment from Edvardsen et al. (2016) using the "-add fragments" algorithm in *mafft* (v7.427; Stamatakis, 2014). The resulting alignment containing haptophyte ASVs and reference sequences was then used to generate a Maximum Likelihood phylogenetic tree with the RAxML program (v8.2.12) with 1000 bootstrap replications. Based on the phylogenetic analysis, the total of 98 ASVs placed in the *Chrysochromulina* clade were extracted from the original haptophyte selection. The initial selection of *Chrysochromulina* ASVs was aligned and screened for possible chimeric sequences by in-depth inspection of their alignment, and by accessing the NCBI BLAST tool for detection of chimeric fragments. This analysis detected 21 chimeric ASVs that were removed from the ASV dataset, and the remaining 77 verified *Chrysochromulina* ASVs were used in subsequent analyses.

The total nanoplankton protist dataset was normalized to even sample sizes with the 'rarefy_even_depth' function in the phyloseq package to its minimum sample size (48,970 reads) yielding 2768 ASVs (61 post-rarefaction *Chrysochromulina* ASVs).

2.6. Isolation and culture of C. leadbeateri

Plankton samples collected during the bloom from Balsfjorden and the Tromsø area were subjected to multiple attempts to isolate *C. leadbeateri* into monoculture. A strain was finally isolated and cultured from a surface seawater sample with a high density of *C. leadbeateri* cells collected offshore of Tromsøy island (69.6469 °N; 18.862667 °E) on 25 May 2019. The sample was transferred through a six-step serial dilution series with the final step having 10^6-fold lower *C. leadbeateri* cell density than the initial sample. Dilution cultures were grown in IMR 1/2 medium (Eppley et al., 1967) with addition of 10 nM selenite (Edvardsen and Paasche, 1992) at salinity 30. Each dilution

sample was cultured in 10 mL borosilicate glass tubes at 4 °C at low photon flux density (10–20 µmol $m^{-2} s^{-1}$) on a 14:10 h light-dark cycle. After periodic examination of cell growth by light microscopy, a *C. leadbeateri* monoculture was established from one of the dilution series. The stock monoclonal isolate was maintained in a temperature-controlled culture room at 13 °C, and eventually deposited in the Norwegian Culture Collection of Algae (NORCCA; norcca.scroll.net) as strain number UIO 393.

2.7. Morphological species identification by electron microscopy

For scanning electron microscopy, a sample collected in Balsfjorden (69.401917 °N 19.03025 °E), was preserved in 1% glutaraldehyde (Sigma-Aldrich, St. Louis, MO, USA), rinsed in sterile filtered seawater and dehydrated in an ethanol series (one rinse in 50, 70, 90 and 96% and four rinses in 100% ethanol). The samples were mounted on poly-L-lysine-coated (Sigma-Aldrich, St. Louis, MO, USA) glass slides before critical point drying (BAL-TEK CPD 030 Critical Point Dryer, Balzer, Liechtenstein). The cover slips were mounted on stubs, then sputter-coated with 7 nm platinum using the Cressington Coating System 308R with 100 W sputter supply 308R and thickness monitor mtm1030R (Cressington Scientific Instruments, Watford, UK). Specimens were examined and photographed with a Hitachi S-4800 Field Emission Scanning Electron Microscope (Hitachi, Tokyo, Japan).

Transmission electron microscopy was conducted on drops of sample placed on formvar and carbon-coated copper grids and fixed in the vapor of 1% osmium tetroxide (Sigma-Aldrich, St. Louis, MO, USA). Fixed mounted specimens were rinsed in distilled water and then exposed to saturated uranyl acetate (Sigma-Aldrich; St. Louis, MO, USA) for contrast. Examination and photography of specimens was performed with a JEOL 1400 plus transmission electron microscope (JEOL, Tokyo, Japan).

2.8. Sanger sequencing of C. leadbeateri strains uio 393 and uio 035

A 30 mL volume of dense cultures of *C. leadbeateri* reference strains UIO 393 and UIO 035 from NORCCA were pelleted by centrifugation at 4000 g for 10 min. DNA was extracted from the pellet with the Nucleo-Spin Plant II kit (Macherey-Nagel, Düren Germany) by cell lysis with Buffer APL1 according to the manufacturer's protocol. To amplify the 18S rRNA marker gene, PCR reactions were run with primers 1F (AACCTGGTTGATCCTGCCAGT) and 1528R (TGATCCTTCTGCAGGTT-CACCTAC) at an annealing temperature of 55 °C in a program of 32 cycles. Direct Sanger sequencing with the two terminal and two additional internal sequencing primers was used to assemble near-full length 18S rRNA gene sequences. The variable D2 and D3 domains of the 28S rRNA gene and the Internal Transcript Spacer (ITS) region were amplified with primers D1R-F (ACCCGCTGAATTTAAGCATA) and D2C-R (CCTTGGTCCGTGTTTCAAGA), and ITSa (CCAAGCTTCTA-GATCGTAACAAGGHTCCGTAGGT) and ITSb (CCTGCAGTCGACA-KATGCTTAARTTCAGCRGG), respectively. Both genes were PCR-amplified at a primer annealing temperature of 52 °C with 32 cycles and Sanger-sequenced from PCR products. The edited sequences were deposited in GenBank under the accession numbers AM491017, AM850687.

2.9. Phylogenetic placement of Chrysochromulina sequences and ASVs

Detailed phylogenetic placement of *Chrysochromulina* ASVs was based on 40 selected ASVs with total read number >100. The ASVs were added into an 18S rRNA gene alignment of reference sequences from the Prymnesiales clade (Edvardsen et al., 2016) that also included the 18 s rRNA gene sequence of cultured strain UIO 393 and three outgroup haptophyte sequences (*Isochrysis galbana, Coccolithus pelagicus,* and *Phaeocystis pouchetti*). The "-add fragments" algorithm in *mafft* (v7.427; Stamatakis, 2014) was used for this step. After final alignment of

Chrysochromulina ASVs with reference Prymnesiales sequences, and selected three outgroup sequences, a Maximum Likelihood phylogenetic tree was generated in the RAxML program (v8.2.12) with 1000 bootstrap replications.

2.10. Statistical analyses

Statistical analyses and plotting of data were performed in R software v.3.6.1 (R Core Team, 2020) using multiple R packages. Unique and shared *Chrysochromulina* ASVs present in each fjord system were identified by creating and visualizing a fjord intersection matrix with the 'upset' function in the UpSetR package (Conway et al., 2017).
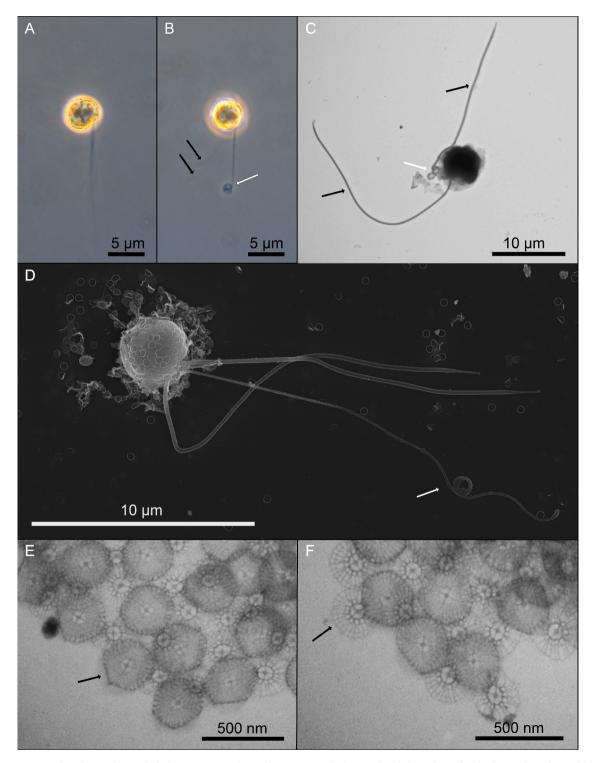

Fig. 2. Light (A-B), scanning-electron (D), and whole-mount transmission-electron (C, E-F) micrographs of *Chrysochromulina leadbeateri* from the studied area. Living cell of cultured strain UIO 393 from offshore of Tromsøy island showing: **A)** chloroplasts and two flagella; **B)** coiling haptonema; **C)** fixed cell with two smooth flagella (black arrows) and a coiling haptonema (white arrow) (6000x magnification). *C. leadbeateri* from a field sample collected in Balsfjorden: **D)** cell with scale cover, flagella and haptonema (5000x magnification); **E)** outer- layer scales (arrow) (20000x magnification); **F)** inner layer scales (arrow) (20000x magnification).

The *Chrysochromulina* community data set was first Hellinger-transformed as recommended for ordination of species abundance data (Legendre and Gallagher, 2001) with the 'decostand' function to obtain a beta-diversity matrix. The 'vegdist' function was subsequently used to compute Bray-Curtis dissimilarities (R. Bray and Curtis, 1957) in vegan package (Oksanen et al., 2020). Permutational multivariate analysis of variance (PERMANOVA) and Distance-based redundancy analysis (dbRDA) on Hellinger-transformed data were then performed with the "adonis" and "dbrda" functions to explore the relationship between the *Chrysochromulina* community composition and environmental variables.
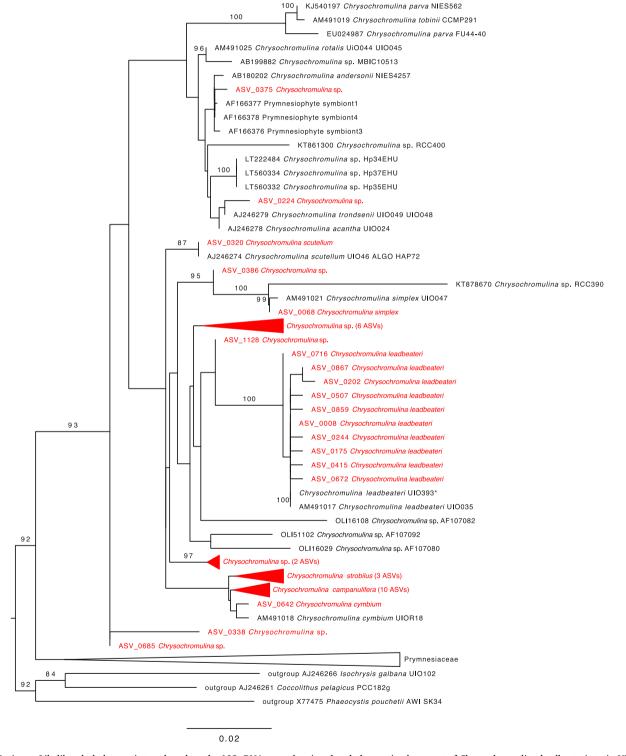

Fig. 3. Maximum Likelihood phylogenetic tree based on the 18S rRNA gene showing the phylogenetic placement of Chrysochromulina leadbeateri strain UIO 393 (marked with *) and the 40 most abundant Chrysochromulina ASVs from the metabarcoding dataset (marked in red) within the 18S rRNA gene reference clade for Prymnesiales (Edvardsen et al. 2016.). Only bootstrap values >80 are shown. Chrysochromulina clades other than C. leadbeateri with two or more ASVs are collapsed. Scale bar represents the number of nucleotide substitutions per site.

2.11. Chrysochromulina abundance and distribution of associated fish kills

During the *Chrysochromulina* bloom in northern Nordland and Troms counties, an emergency group led by the Fisheries Directorate of Norway was established to monitor the bloom and advise fish farmers regarding bloom spreading and risk of fish mortalities. Light microscopy cell counts of *Chrysochromulina* available from the emergency group focusing on sites with fish kills were compiled by the Norwegian Institute of Marine Research (IMR) to provide an overview of the coordinated field sampling and to advise the fish farmers. Data from this monitoring activity was analyzed and is presented herein for regional comparison with the spatio-temporal distribution of blooms obtained from the HE533 oceanographic expedition in northern Norwegian waters.

3. Results

3.1. Morphology-based identification of Chrysochromulina leadbeateri

A haptophyte belonging to the genus *Chrysochromulina* (Lackey, 1939) was identified by light microscopy from samples of the bloom collected in Balsfjorden. The bloom flagellate exhibited morphological features typical of *C. leadbeateri* Estep, Davis, Hargreaves & Sieburth (Estep et al., 1984) (Fig. 2A, B, C and D). Cells were small, ~5 μm in diameter, with two yellow-brown chloroplasts and two equal flagella. The prominent haptonema was slightly longer than the flagella, with the ability to coil and extend. Live cells exhibited characteristic active swimming behavior for *Chrysochromulina*, with frequent changes of direction and fast rotation around the central point of the cell. Detailed morphological observations by scanning- (SEM) and transmission (TEM) electron microscopy revealed typical organic scales covering the cells (Fig. 2D, E, F), which are unique for each haptophyte species. Under TEM, the morphology of these scales appeared as characteristic for *C. leadbeateri*, with distinct inner- (Fig. 2E) and outer- (Fig. 2F) layer organic scales.

3.2. Phylogenetic placement and genetic diversity of Chrysochromulina leadbeateri

The archived gene sequences of 18S rRNA and the variable D1 and D2 domains of 28S rRNA (AM491017, AM850687) of *C. leadbeateri* UIO 035, isolated from the Vestfjorden bloom in 1991, were confirmed by re-sequencing the strain. The 18S and 28S rRNA gene sequences of *C. leadbeateri* UIO 393 from the bloom near Tromsøy island were identical to those of *C. leadbeateri* UIO 035. The ITS rRNA sequences of the two strains showed some degree of sequence polymorphism and/or intragenomic variation, but they were also largely consistent (data not shown).

Among the 40 most abundant ASVs placed within the *Chrysochromulina* clade, 10 ASVs were grouped with *C. leadbeateri* UIO 393 and UIO 035 with high bootstrap value (Fig. 3). The V4 region of the 18S rRNA gene of the most abundant variant (ASV_008) was identical to those of UIO 393 and UIO 035.

3.3. Diversity and distribution of Chrysochromulina genotypes based on metabarcoding data

Phylogenetic analysis of the 40 most abundant *Chrysochromulina* ASVs revealed unexpectedly high intrageneric and infraspecific genetic diversity in the studied fjord systems of northern Norway (Fig. 3). Six ASVs corresponded to described species and eight additional distinct clades were identified, representing at least 14 genotypes and putative *Chrysochromulina* species. *C. leadbeateri* and *C. campanulifera* clades contained 10 ASVs each, whereas *C. strobilus* contained two ASVs and *C. simplex*, *C. scutellum* and *C. cymbium* contained only one distinct ASV.

Chrysochromulina sequence variants (ASVs) were detected in all samples but their absolute abundances were typically low, ranging between $n = 68$ at St 17 and $n = 1956$ at St 23, except in Balsfjorden (Fig. 4). *C. leadbeateri* ASVs were absent only from the innermost station in Porsangerfjorden (St 17) and were dominant in the Balsfjorden bloom. The *C. leadbeateri* sequence read abundances in Balsfjorden ranged between 6833 and 28,147, with highest numbers found at the inner stations St 09 and St 10, where they dominated all nanoplankton. Detailed analyses of these ASV abundance patterns in the nanoplankton size-fraction among all the fjord systems showed the clearest dominance of *C. leadbeateri* in Balsfjorden during the sampling period (Fig. 5). A minority of *Chrysochromulina* ASVs (14 out of 61) were present at all stations (Fig. 5); endemicity was highest in Vesterålen (12 unique ASVs) and even the Balsfjorden bloom contained three ASVs not observed in other fjord systems.

3.4. Distribution and cell abundance of C. leadbeateri

The abundances of *C. leadbeateri* inferred by different qualitative and quantitative methods showed a high degree of correspondence (Fig. 6; Supplementary Fig. 1) for both bloom and non-bloom fjord states. Linear regression analyses for the combined data from light microscopy counts, flow cytometry detection of *Chrysochromulina*-like cells, and absolute read numbers of *C. leadbeateri* ASVs from 18S rRNA gene metabarcoding yielded $r^2 > 0.93$. In non-bloom areas of Vesterålen, Lyngen and the northern Finnmark fjords, flow cytometry estimates for the *Chrysochromulina*-like population cell densities in the surface layer were consistently $< 5 \times 10^3$ cells L^{-1}. With few exceptions (e.g., outer parts of Lyngenfjorden), similar abundances, of typically $< 10^4$ cells L^{-1}, were determined by light microscopy counts in the non-blooming areas.

The highest cell abundances (27.6×10^6 cells L^{-1}) of *C. leadbeateri* among the fjord systems, as determined by light microscopy counts, were found in Balsfjorden. This corresponded with the highest signal (28.3×10^6 cells L^{-1}) detected in the small nanoeukaryotes-gate (Nk2) (referred to as the *Chrysochromulina*-like population) in the flow-cytometry analysis. The clear signature in gate Nk2 enabled near real-time tracking of *Chrysochromulina*-like nanoflagellates, as well as clusters of other plankton groups, in samples collected throughout the study area. The nearly monospecific *C. leadbeateri* bloom, as indicated by light microscopy, formed a sharp discrete patch in samples analyzed by flow cytometry from Balsfjorden at St 10 (Suppl. Fig. 1). High cell abundance of the *Chrysochromulina*-like population detected at St 9 by flow cytometry (21.4×10^6 cells L^{-1}) could not be confirmed by light microscopic cell counts due to missing data from that station. However, similar ASV read abundance data for *C. leadbeateri* suggests that *Chrysochromulina* cell densities were indeed similar at St 9 and St 10.

Aggregated data from the Institute of Marine Research (IMR), Norway derived from the Norwegian regional emergency monitoring program on fish-killing blooms is shown in Fig. 7. During the weeks 20 and 21 (13–26 May) of 2019, most bloom observations came from the northern part of Nordland and southern Troms, with an ongoing high-magnitude *C. leadbeateri* bloom in Vestfjorden (Nordland) and Astafjorden (Troms) (for geographic orientation see Fig. 1). From 27 May- 2 June high cell abundances were also registered in Balsfjorden, Malangen, and around Tromsø (Fig 7B). In week 23 (3–9 June) there was still a persistent bloom in the Vestfjorden area, but also high cell abundances registered at the outer coast of Troms county (Fig. 7C).

3.5. Association of Chrysochromulina with abiotic factors and prokaryotes

The RDA plots illustrate correlations of specific abiotic conditions (Fig. 8A) and major prokaryotic groups (Fig. 8B) with high abundances of all *Chrysochromulina* ASV reads. The Balsfjorden stations yielded the highest proportion of *Chrysochromulina* reads. Temperature and dissolved inorganic nutrients nitrate and phosphate were positively correlated, whereas salinity was negatively correlated with abundance
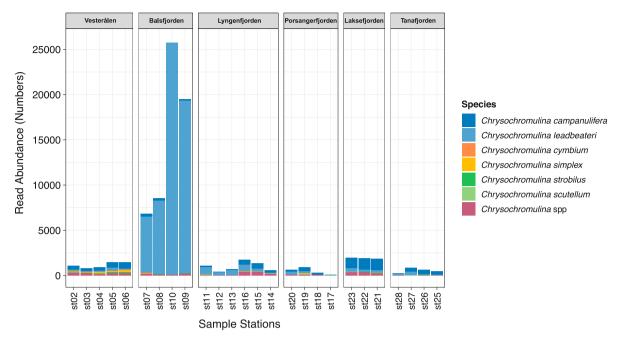
Fig. 4. Aabsolute read abundances of ASVs assigned to all *Chrysochromulina* species detected at different oceanographic stations after subsampling to the minimum sample size.
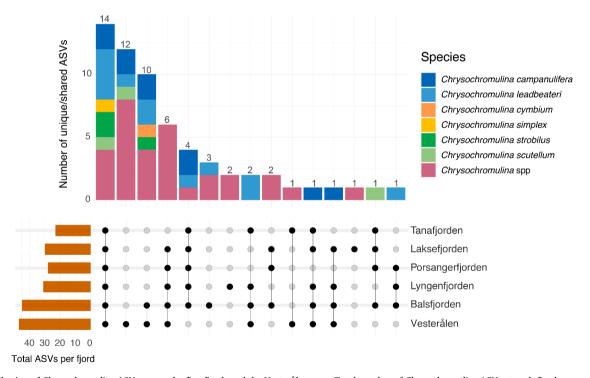

Fig. 5. Distribution of *Chrysochromulina* ASVs across the five fjords and the Vesterålen area. Total number of *Chrysochromulina* ASVs at each fjord or area is shown to the left (orange bars). The vertical bars indicate the number of *Chrysochromulina* ASVs unique to a particular fjord (single dark circles) or shared among fjords (dark circles connected by solid lines), as well as the species representation by color codes.

of *Chrysochromulina* taxa (Fig. 8A). PERMANOVA results indicate, however, that only temperature and salinity ($p = 0.013$, $R^2 = 0.093$, and $p = 0.004$; $R^2 = 0.138$, respectively) (Supp. Table 2) were significantly correlated with *Chrysochromulina* variation across samples (red vectors in Fig 8A), explaining 23.1% of the total variability.

Multivariate redundancy analyses for *Chrysochromulina* and prokaryotic groups showed high spatial variation in microbial composition (Fig. 8B). Proteobacteria dominated the bacterioplankton at all stations,

with average ASV read abundances of 68% of the total sequence variants. Within Proteobacteria, the orders Alteromonadales, Rhodobacterales, Oceanospirillales, Cellvibrionales and the SAR86 clade were especially prominent.

Comparison of bacterial correlations at the generic level against *Chrysochromulina* ASVs revealed 146 significantly positive and 26 negative correlations for Alphaproteobacteria; 88 positive and 27 negative for Flavobacteriales; and 136 and 68 for
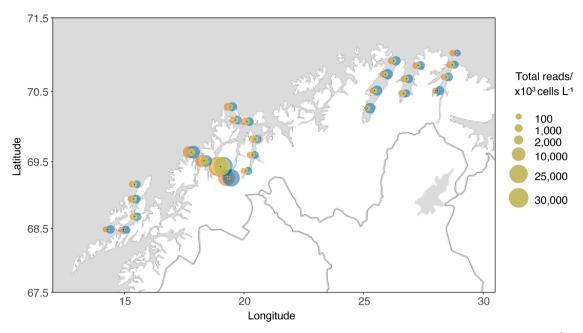
Fig. 6. Abundance of *C. leadbeateri* cells collected on oceanographic transects from surface waters and compared by light microscopy counts (x10^3 cells L^{-1}; yellow circles), flow cytometry estimates of the *Chrysochromulina*-like populations (x10^3 cells L^{-1}; blue circles) and total metabarcoding read numbers (red circles) of ASVs identified as *C. leadbeateri* in the nanoplankton size-fraction. The "x" symbol indicates that no *Chrysochromulina* cells were detected by the respective method, except in the case of the innermost station of Balsfjorden, for which light microscopy cell count data are missing.
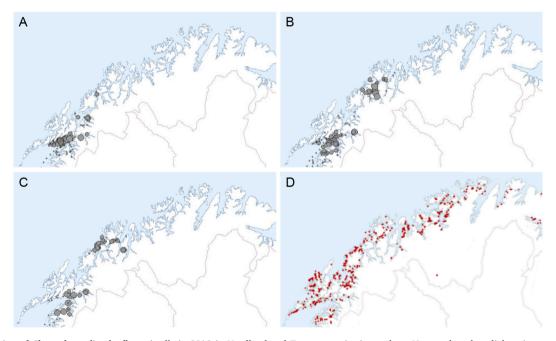

Fig. 7. Distribution of *Chrysochromulina leadbeateri* cells in 2019 in Nordland and Troms counties in northern Norway based on light microscopy cell counts of integrated samples from 0 to 2 m depth. Small dots (<10^6 cells L^{-1}; medium-size dots (1–5 × 10^6 cells L^{-1} and large dots (>5 10^6 cells L^{-1}). Maps A-C show the cell distribution based on data collected by the Norwegian emergency bloom monitoring group during weeks 20–21, 22, and 23, respectively. Map D shows salmon aquaculture farm locations in the region (data from the Directorate of Fisheries of Norway, with permission).

Gammaproteobacteria, respectively (Supplementary Fig. 3, 4, 5, Supplementary Table 2). These comparisons include, for example, negative correlations of *Chrysochromulina* ASVs to the OM43 clade, and positive correlations to the bacterial genera *Colwellia, Vibrio, Shewanella, Psychromonas, Allivibrio, Psychrobium* and *Candidatus endobugula* (all Gammaproteobacteria). Among Alphaproteobacteria, *Lentibacter* correlated negatively against four *Crysochromulina* ASVs while *Constrictibacter, Holosporaceae, Pseudorhodobacter*, Rhizobiales and Acetobacteraceae correlated positively with each 9 *Crysochromulina* ASVs. The

Flavobacteriales genera *Polaribacter* and marine groups NS2b and NS4 all correlated negatively to *Chrysochromulina* ASVs. Conversely, *Winogradskyella, Lutibacter, Maritimimonas* among others, were positively correlated with several *Chrysochromulina* ASVs.

3.6. Oceanographic conditions and advective processes affecting bloom distribution

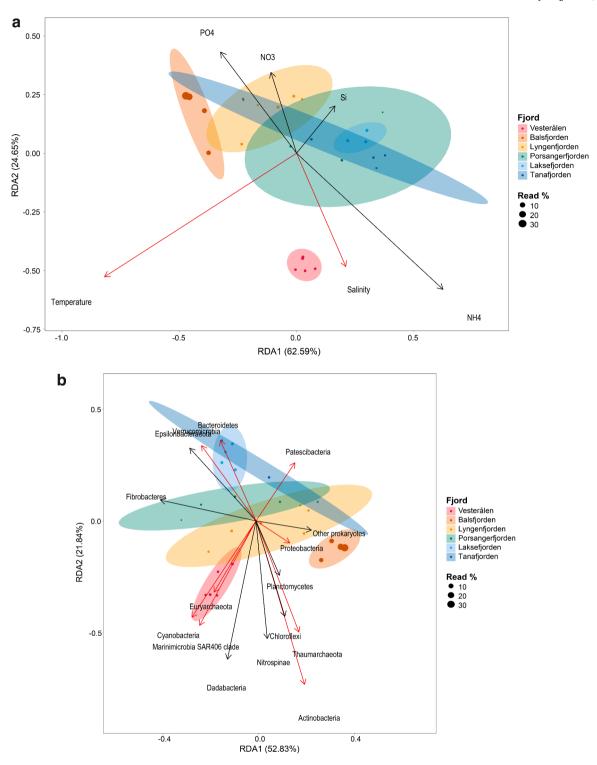During the bloom period the upper waters of the studied fjord

Fig. 8. Redundancy analysis plots showing relative abundances of *Chrysochromulina* ASVs in relation to: **A)** environmental factors and **B)** prokaryotic phyla detected by metabarcoding within the studied fjord systems. Each field sample is represented by a dot proportional in size to relative *Chrysochromulina* ASV read abundances. Distance between the points shows degree of similarity of the nanoplankton composition, while direction and length of the eigenvectors (arrows) indicates correlation of abiotic factors and prokaryotic ASV reads with abundance of *C. leadbeateri* signatures. Eigenvectors of factors with p-value <0.05 are marked in red.

systems were characterized by less saline waters with highest temperature near the surface. Within Balsfjorden the salinity ranged between 32 and 35, and temperature varied from 3 °C in deep water below 120 m to 8.5 °C at the surface (Fig. 9). The inner section of the Balsfjorden system exhibited a distinct chlorophyll maximum in surface waters just above the thermocline (e.g., 12 m at St 10) corresponding to the pycnocline layer with the highest *Chrysochromulina* cell abundance.

Based on an 800 m grid model (IMR, NorKyst800, Albretsen et al. 2011) (Fig. 10), the prevailing sea current in northern Norway flows from south to northeast along the open coast. Offshore of Troms county the current divides into two branches, one proceeding further north up to Svalbard and the other flowing along the coast of Finnmark.
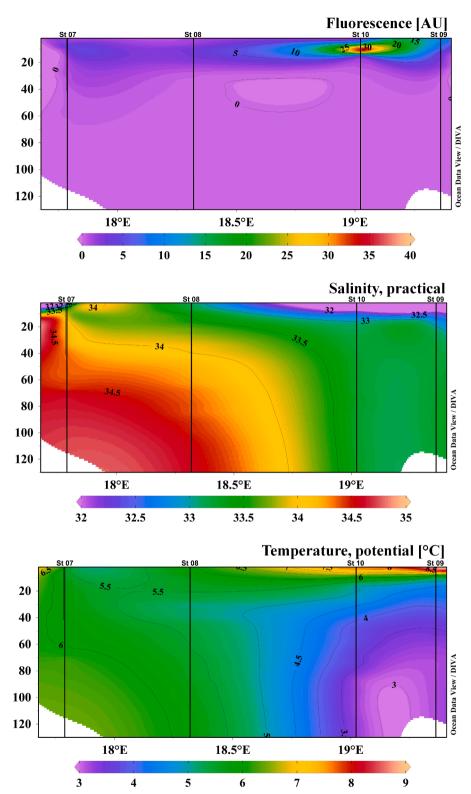
Fig. 9. Balsfjorden. Depth-longitudinal sections in Balsfjorden for chlorophyll fluorescence [arbitrary units, AU], salinity and temperature [°C]. Data are shown from the outer to the inner fjord; stations 7 to 10 are marked as black lines.

4. Discussion

The investigation of the *C. leadbeateri* bloom during the research cruise from Vesterålen to Tanafjorden in northern Norway roughly coincided with the spatio-temporal distribution of the bloom in areas subjected to major salmon kills. *Chrysochromulina* blooms initiated within the fjords in late spring are expected to be advected according to

the typical fjord circulation pattern, with surface current flows from the inner fjords towards the open coast following the density gradients of the respective water masses. The recently isolated bloom-forming *C. leadbeateri* strain UIO 393 was morphologically and genetically identical for three independent loci at the species level to strain UIO 035 from the fish killing bloom in Vestfjorden in Lofoten, Nordland in 1991 (Edvardsen et al., 2011). In any case, among the *Chrysochromulina*
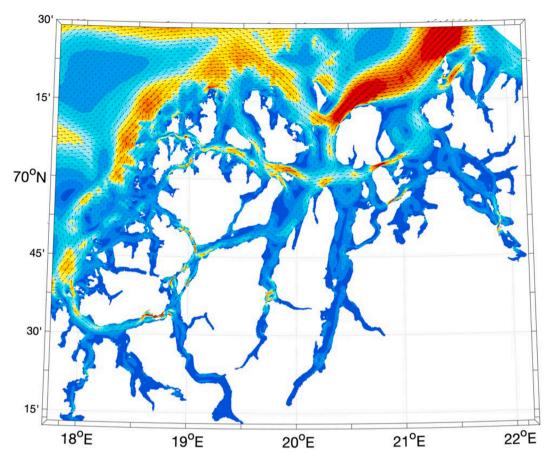
Fig. 10. Annual average surface (0 m) currents in the study area based on the NorKyst800 model (Albretsen et al., 2011). Arrows represent the current direction and strength; colors indicate current speed, where red is high (>0.3 m s^{-1}) and blue indicates low (<0.05 m s^{-1}) speed. (Source: Jon Albretsen Institute of Marine Research (IMR), Norway,).

variants identified in this study, only *C. leadbeateri* is known to cause harmful blooms associated with fish kills in Norwegian waters.

4.1. Species identification and phylogenetic associations

Detailed analysis of the 18S rRNA gene metabarcoding data set also revealed a high putative species-level diversity of *Chrysochromulina* ASVs in the studied fjord systems. The 14 well supported clades likely represent distinct *Chrysochromulina* species. Nevertheless, only six of them are phylogenetically defined by reference sequences, with high intraspecific diversity observed in *C. campanulifera* and *C leadbeateri*. A further eight *Chrysochromulina* species were provisionally identified from these field populations based on their morphology alone but uncertainty remains because reference rRNA gene sequences are not available for some of them. These eight unassigned *Chrysochromulina* clades may indeed represent new species that lack reference sequences, but they may also merely reflect cryptic plastic morphological features. Since only the 40 most abundant ASVs were analyzed in detail, higher genetic diversity in these samples may have gone unappreciated.

Metabarcoding revealed the identity and distribution of *C. leadbeateri* across fjord systems in northern Norway, effectively pinpointing peak abundances of *C. leadbeateri* within massive blooms. The V4 18S rRNA gene marker also proved efficient in confirming the distributional patterns of all *Chrysochromulina* species even at sub-bloom cell densities, as well as their species-level and infraspecific diversity. The number of detected *Chrysochromulina* ASVs (or even "species") would be expected to be even higher with a greater sequencing depth, or by targeting the 28S rRNA gene (Gran-Stadniczeňko et al., 2017) or the ITS rRNA region. Furthermore, alternative higher-resolution molecular markers such as microsatellites would give a more differentiated and

diverse view of the infraspecific or even population level genotypic diversity within *C. leadbeateri* (Godhe et al., 2016; Ruggiero et al., 2017; Wolf et al., 2021).

4.2. Biogeography and spatio-temporal distribution

After the first week in June, high cell counts of *C. leadbeateri* were no longer registered from Balsfjorden, but higher cell abundances were found west and northwest of Tromsø. *Chrysochromulina leadbeateri* was present at low to moderate ($<10^4$ cells L^{-1}) cell densities over a larger area north of Lofoten during the entire sampling period. Unfortunately, detailed monitoring data on the extent and magnitude of the *Chrysochromulina* bloom were not available after the bloom event and cell counts from the northern areas are missing. This lack of biogeographical information makes it difficult to track the progression and succession of the "bloom". Or in fact to ascertain if this represents a unique spreading event rather than multiple uncoordinated blooms developing independently in different fjord systems.

Comparison of the fish-killing *C. leadbeateri* event in 1991 with bloom dynamics and distribution from 2019 reveals striking similarities but also distinctive biogeographical features. During the 1991 event, *C. leadbeateri* was present over a large region of northern Norway from Vestfjorden to Varanger (Hegseth and Eilertsen, 1991), but only at sub-bloom cell densities ($<0.5 \times 10^6$ cells L^{-1}) outside the peak bloom areas. In comparison, in the 2019 event, *Chrysochromulina* species were also recorded throughout the entire region, but only at low cell densities ($<10^4$ cells L^{-1}) in Finnmark and Troms county. The authors (Hegseth and Eilertsen, 1991) of the previous study concluded that *C. leadbeateri* was a typical and common member of the phytoplankton community in northern Norway during the post-spring bloom period May-June.

Routine phytoplankton monitoring in 2019 prior to and after the fish-killing bloom event also confirms that *Chrysochromulina* species are a consistent presence in the phytoplankton community in this region, at least from April – June (via L-J. Naustvoll; „Algestatus.hi.no" in Norwegian; data not publicly available).

The role of hydrodynamics in determining the spatial distribution of *Chrysochromulina* blooms beyond the mesoscale (>10 km) cannot be precisely attributed for specific events because of insufficient in situ data. Nevertheless, based on the general current velocities and trajectories modelled for the region (Fig 10), a bloom forming in the outer part of the fjords in southern Troms county could be transported further north and east, thereby affecting a larger area in Finnmark. The two major *Chrysochromulina* blooms recorded in 1991 and 2019 and associated with fill-kills were most likely initiated within the fjords (e.g., Ofotfjorden, Astafjorden, and Balsfjorden in the 2019 case) and then transported in the surface layer to the outer parts of the fjord systems. Phytoplankton monitoring during the 2019 bloom event in Troms showed a plausible transport out of Malangen and then northward along the outer coast of Kvaløya island, following the general current pattern (Fig. 10), before the bloom decreased in intensity. The dominant prevailing currents in the area may also account for transport of *Chrysochromulina* from the outer part of Balsfjorden to Lyngen. It is, however, unlikely that the bloom(s) in Ofotfjorden and Astafjorden were transported all the way to Balsfjorden or Malangen within the bloom succession cycle.

An alternative scenario for the temporal and spatial distribution of C. *leadbeateri* and associated blooms, is supported by the synoptic field sampling in 2019. In this scenario, this species was likely present at low cell densities throughout the fjord systems in the region, generating endogenous blooms in environmentally favorable circumstances. That a single incipient bloom population was advected and transported from an initiation zone throughout the entire region is less consistent with the time-scale of appearance of local bloom events in multiple locations, given prevailing current velocities and trajectory (refer to Fig. 10). If *C. leadbeateri* was already present at low cell densities over a wide biogeographical range, these could serve as local seed populations for development of virtually monospecific blooms subject to selection based on sub-mesoscale environmental conditions and community interactions. In the 1991 event, the presence of *Chrysochromulina* in eastern Finnmark did not correspond with putative transport of cells from the bloom area in Vestfjorden (Hegseth and Eilertsen, 1991). Furthermore, no monitoring data or reports of fish mortalities in the 2019 event support the interpretation of mass transport the *C. leadbeateri* bloom in Vestfjorden/Astafjorden to the fjords further north. This favors the hypothesis that local environmental factors were primarily responsible for initiation and development of the blooms, although perhaps reinforced by spreading to northern areas due to advective transport over longer (weeks) time-scales.

4.3. Changing environmental parameters as drivers of bloom dynamics

Massive blooms of *Chrysochromulina* only occur sporadically in Norwegian coastal waters. *C. leadbeateri* formed major fish-killing blooms in 1991 and 2019, but only minor blooms in 1998, 2003 and 2009 in the study area (W. Eikrem, unpublished data; Karlson et al. 2021). There is still no full synthesis of environmental factors underlying the formation of these blooms.

In fact, the rarity of major fish-killing events linked to *Chrysochromulina* or other ichthyotoxic haptophytes in Norwegian waters over the past three decades (HAEDAT 2021; Karlson et al. 2021) poses a considerable challenge to defining patterns in causal mechanisms and bloom dynamics. *Chrysochromulina* species are common members of the phytoplankton community all along the coast of Norway (Elianne S. Egge et al., 2015a, 2015b; Gran-Stadniczeňko et al., 2017; Johannessen et al., 2017). Such species are often present throughout most of the year albeit often in background cell densities but usually with a peak during summer (Lekve et al., 2006).

This current *Chrysochromulina* study indicates a positive correlation with reduced salinity and increasing temperature. Hegseth and Eilertsen (1991) also found a relationship between high cell densities of *Chrysochromulina* and reduced salinity, but not with temperature, during the 1991 bloom. Unfortunately, there is little information on the temperature optima or tolerance limits for growth of *C. leadbeateri* under controlled conditions. Except for measurements of ambient environmental parameters during the bloom there are only incomplete field data to support reconstructions of environmental regimes through the bloom succession processes.

In fjord systems, changes in salinity in the surface layer due to river runoff affect the vertical stability of the water column. Lowering salinity increases the stability of the water column and low wind stress further reduces vertical mixing. During both the 1991 and 2019 Chrysochromulina bloom, lower salinity was correlated with bloom intensity. Nevertheless, *Chrysochromulina* bloom dynamics are not driven by salinity gradients alone. Prevailing meteorological conditions such as wind stress and cloud cover can also affect phytoplankton dynamics and productivity (Wells et al., 2015). Generally, a succession of warm days after relatively high input of terrestrial nutrients to the fjords by heavy rainfall during a short time promotes blooms of small haptophytes, such as *C. leadbeateri* (Rey, 1991). There are similarities in the meteorological conditions during spring in 1991 and 2019, prior to the *C. leadbeateri* bloom events. At the start of the *Chrysochromulina* blooms, the weather was sunny and with relatively low wind stress in both years (Rey, 1991, Meteorological institute: www.seklima.met.no). Furthermore, in both bloom event cases there were high levels of river run-off in advance of the bloom, lowering the salinity in the surface layer and presumably bringing exogenous nutrients and organic material to the surface layers. In combination with clear skies and thus high solar irradiance, and abundant available nutrients in the upper mixed layer, such conditions favor small, mixotrophic flagellates with high growth rates.

The environmental data from the cruise HE533 and the distribution and abundances of *C. leadbeateri* based on the relative ASV sequence read numbers during late May to early June 2019 highlight the potential role of higher temperatures and lower salinity in vertical partitioning and distribution of the bloom in specific fjords. The abundance of *C. leadbeateri* showed positive correlations with temperature, negative correlation with salinity, and a slightly positive correlation with phosphate and nitrate. Detailed analysis of the vertical distribution of the bloom in Balsfjorden shows a clear abundance peak defined by chlorophyll near the pycnocline (about 12 m depth at St 10), but does not explain if this patch represents physical stratification due to the sharp density gradient or aggregation behavior at the nutricline.

Climate change scenarios for the north eastern Atlantic and adjacent North Sea and Norwegian Sea predict future increases in annual precipitation and seasonal rainfall intensity in the region. Coupled with increasing surface water temperature and more prolonged and intense atmospheric heatwaves in summer, this increased runoff in coastal regions should lead to enhanced stratification and reduced vertical mixing within fjord systems. In addition to the hydrodynamic effect of increased freshwater runoff in creating a sharper pycnocline and decreasing salinity in the surface layer, increased freshwater runoff will enhance transport of nutrients and organic components to the coastal ocean (IPPC2021, Zhongming et al., 2021). In the Norwegian Sea and adjacent waters of the Barents Sea, this regime shift should confer a competitive advantage of motile mixotrophic haptophytes such as *Chrysochromulina* over diatoms in the phytoplankton community. Although such climate-driven effects on *Chrysochromulina* bloom dynamics are not yet apparent for the Norwegian Sea, blooms of other Prymnesiales species have been reported further south in the Skagerrak under these bloom-promoting conditions (Dahl et al., 2005). The increasing risk for high magnitude extensive blooms of *C. leadbeateri* causing fish mortalities is consistent with historical data from the region and suggests enhanced risk of bloom spreading to sub-arctic and arctic areas within

decades to come.

4.4. Biotic interactions defining chrysochromulina bloom dynamics and community structure

Many and perhaps all haptophytes are mixotrophs (Jones et al., 1994), but especially members of the genera *Prymnesium*, *Haptolina* and *Chrysochromulina*. Changes in inorganic nutrient supply and N:P ratios are therefore key factors regulating species competition and may even affect the toxicity of certain haptophyte species (Edvardsen and Paasche, 1998). Associated bacterial communities may benefit from the high biomass haptophyte bloom and utilize leaked or excreted algal metabolites for heterotrophic growth, particularly in the climax and senescence bloom phases. Finally, particulate- and dissolved organic matter (POM and DOM, respectively) released from lysed plankton competitors and mass mortalities (fish, etc.) elicited by the massive *C. leadbeateri* bloom may further sustain and promote heterotrophic bacterial growth in species-specific associations on different spatio-temporal scales in diverse fjord systems.

The extent to which microplankton grazing and phagotrophy regulate bloom dynamics and successional processes remains to be determined for *Chrysochromulina* and other haptophytes in natural populations from temperate fjord systems. Metabarcoding analyses of the prokaryotic diversity and distribution in the study area of the Norwegian Sea served only to identify co-occurrence patterns with bacteria. Such co-occurrences might result from similar responses to environmental drivers or to food web interactions such as bacterial ingestion by *C. leadbeateri* (phagotrophy). While negative correlations could reflect high phagotrophic activity upon bacterial prey or negative allelochemical responses, these interactions would need to yield taxon-specific consequences to be detectable by metabarcoding analysis.

The greater magnitude of positive correlations of *Chrysochromulina* abundance with bacterial genera compared to the low number of negative correlations reflect mostly bacterial opportunists of the Gammaproteobacteria, Flavobacteriales and Alphaproteobacteria. These groups are often associated with phytoplankton blooms (Buchan et al. 2014) and such bacterioplankton could affect successional processes and bloom dynamics (Teeling et al., 2012, 2016). Marine Flavobacteria are common degraders of high molecular- weight organic matter derived from phytoplankton (Buchan et al., 2014) and Alteromonadales and Rhodobacterales are considered primary remineralizers of particulate carbon in the oceans (Kong et al., 2021). Bacterial taxa correlations with *C. leadbeateri* likely represent the integrated outcome of complex predation and species-specific growth responses to organic matter availability during the haptophyte blooms. These correlations, however, represent only a static view of species trophic interactions, such as prey selectivity or relative contribution to bloom initiation or sustainability.

Studying a *Chrysochromulina* bloom with respect to bacterial succession dynamics would allow deeper insights into the specific phytoplankton-bacteria interactions. The purely geographical patterns generated by metabarcoding must be interpreted via more detailed ecological studies to understand the associations and dynamics of particular bacterial species and mixotrophic activity of *C. leadbeateri*.

4.5. Chrysochromulina bloom association and consequences of fish mortalities

Historical and recent field observations on the occurrence and abundance of *C. leadbeateri* and related *Chrysochromulina* species over several decades indicate that they are a natural component of the phytoplankton community, but are particularly prominent in late spring (May-June) in northern Norway. There is no evidence that these species are invasive or recently introduced to the region. High magnitude blooms ($>2 \times 10^6$ cells L^{-1}) are rather rare events along the Norwegian coast (Lekve et al., 2006). Nevertheless, those major bloom events that do occur can have devastating consequences on fish aquaculture within

the fjord systems. Most aquaculture operations, particularly for farming salmonids, in northern Norway are situated within or adjacent to the fjords, and are therefore subject to rapid development of HABs within the fjord systems, as well advective transport of massive blooms from adjacent areas. In general, the prevailing current systems in the region flow in a northeast direction along the open coast and from the inner fjords to the outer part, thereby providing an advective mechanism for bloom dispersion over a wide area.

The rapid expansion of aquaculture in northern Norway, particularly of salmon farming, is shown by current high density of farms (Fig. 7D). Hence it is more likely that the increased fish mortalities and socio-economic consequences of *Chrysochromulina* blooms is largely attributable to aquaculture intensity, without necessarily implying a biogeographical expansion of the causative species or blooms. This is reflected in the comparative data for fish mortalities and economic losses from the 1991 versus 2019 *C. leadbeateri* blooms. During the 1991 bloom, approximately 740 t of salmon died, with an estimated value of 3.5 million US\$. Expansion of fish aquaculture in the area by 2019, with more fish farms and higher biomass of farmed salmon, resulted in loss of 14,500 t of salmon due to the *C. leadbeateri* bloom in Troms and Nordland county (event summarized in Marthinussen et al., 2020). These losses are estimated to be 2% of the annual production of farmed salmon at a national level and 6.5% of the annual production in Nordland and Troms. Fourteen companies were affected, losing between 5% and 95% of potential harvest. The economic consequences, direct and indirect gross effect, have been estimated to approximately 280 million US\$, posing a massive loss for the local economy and the Norwegian fish farming industry.

In this context, the *C. leadbeateri* bloom in 2019 caused massive mortality of farmed salmon, but there were no corresponding reports of mortality of wild fish in the bloom areas. Similarly, during the 1991 bloom (Hegseth and Eilertsen, 1991), only one case of mortality of small pollock was reported from Finnmark. This wild fish mortality event was outside the bloom area and only at low *Chrysochromulina* cell densities recorded from phytoplankton samples at the time. In any case, farmed salmon in pens within and adjacent to the fjords are clearly at much higher mortality risk from *Chrysochromulina* blooms than wild fish populations. Caged salmon are subjected to a prolonged longer and more intense exposure to the bloom, as they cannot escape to deeper water below the bloom layer.

Although it was not possible to give a precise lethal exposure of *C. leadbeateri* cells to caged salmon from the 2019 event, cell densities between 1- 2×10^6 cells L^{-1} typically caused changes in swimming behavior, whereas salmon mortalities occurred at $>2–3 \times 10^6$ cells L^{-1} (L-J. Naustvoll, unpubl. data) The exact mechanism of mortality and nature of the ichthyotoxins or other allelochemical interactions that contribute to observed mortalities are still unknown for *C. leadbeateri* blooms.

5. Conclusions

Chrysochromulina leadbeateri was ubiquitous among all stations in northern Norway during the major fish-killing event. The dominance of this species over other nanoplankton within the bloom and high cell abundances coincided spatio-temporally with the mass fish mortalities. This leaves little doubt that *C. leadbeateri* was the primary if not exclusive cause of the fish kills in the 2019 event, although the proximal mechanism of action remains undefined. This association of *C. leadbeateri* with fish kills in northern Norway is supported by metabarcoding analysis and retrospective taxonomic comparison with a cultured strain from the 1991 event. The rarity of these massive fish-killing blooms precludes firm conclusions regarding the initiation and successional processes driving bloom dynamics. High water column stratification, particularly within the fjords, promoted by high land runoff, reduced wind-driven mixing and increasing surface water temperatures are favorable conditions in general for haptophyte blooms.

Such "bloom permissive" environmental regimes can be quickly established on the meso-scale by prevailing meteorological conditions (warm, sunny weather, abundant rainfall and snow melt, etc.). However, such favorable conditions have been observed in other years without apparent blooms in northern Norway. The environmental selection of *C. leadbeateri* as the dominant phytoflagellate is more likely due to biotic factors, such as grazing, nutrient competition and perhaps mixotrophic interactions. This points to the requirement for controlled laboratory experiments on cultured isolates now available and mesocosm studies on such ecophysiological variables. Metabarcoding has been established a viable approach for determining the identity and abundance of fish-killing haptophytes in Norwegian coastal waters. The implementation of such technology into bloom monitoring strategies over wider spatio-temporal scales, will assist in developing scenarios for future bloom dynamics. With particular focus on early warning systems for local fish farm sites, these initiatives will be critical to sustaining the recent expansion of salmonid aquaculture in northern Norway.

Authors' contribution

UJ, LS, AC, SG, BB, and LN designed the study and coordinated the sampling strategy and data analyses. UJ led the organization of the manuscript but all authors were involved in data analyses, contributed to writing, and all reviewed and accepted the final version of the manuscript.

Funding

Declaration of competing interest

The authors declare that they have no known competing financial interests or personal relationships that could have appeared to influence the work reported in this paper.

Acknowledgements

Supplementary materials

Supplementary material associated with this article can be found, in the online version, at doi:10.1016/j.hal.2022.102287.

References

Albretsen, J., Sperrevik, K., Staalstrøm, A., Sandvik, A., Vikebø, F., Asplin, L., 2011. NorKyst-800 Report no. 1: User Manual and Technical Descriptions. Fisken og havet.

Andersen, N., Hansen, P., Engell-Sørensen, K., Nørremark, L., Andersen, P., Lorenzen, E., Lorenzen, N., 2015. Ichthyotoxicity of the microalga *Pseudochattonella farcimen* under laboratory and field conditions in Danish waters. Dis. Aquat. Org. 116, 165–172. https://doi.org/10.3354/dao02916.

Apprill, A., McNally, S., Parsons, R., Weber, L., 2015. Minor revision to V4 region SSU rRNA 806R gene primer greatly increases detection of SAR11 bacterioplankton. Aquat. Microb. Ecol. 75, 129–137. https://doi.org/10.3354/ame01753.

Avrahami, Y., Frada, M.J., 2020. Detection of Phagotrophy in the marine phytoplankton group of the Coccolithophores (Calcihaptophycidae, Haptophyta) during nutrient-replete and phosphate-limited growth. J. Phycol. 56, 1103–1108. https://doi.org/10.1111/jpy.12997.

Bray, J.R., Curtis, J.T., 1957. An ordination of the upland forest communities of southern Wisconsin. Ecol. Monogr. 27, 325–349. https://doi.org/10.1890/1.

Bresnan, E., Arévalo, F., Belin, C., Branco, M.A.C., Cembella, A.D., Clarke, D., Correa, J., Davidson, K., Dhanji-Rapkova, M., Lozano, R.F., Fernández-Tejedor, M., Guðfinnsson, H., Carbonell, D.J., Laza-Martinez, A., Lemoine, M., Lewis, A.M., Menéndez, L.M., Maskrey, B.H., McKinney, A., Pazos, Y., Revilla, M., Siano, R., Silva, A., Swan, S., Turner, A.D., Schweibold, L., Provoost, P., Enevoldsen, H., 2021. Diversity and regional distribution of harmful algal events along the Atlantic margin of Europe. Harmful Algae 102, 101976. https://doi.org/10.1016/j.hal.2021.101976.

Buchan, A., LeCleir, G.R., Gulvik, C.A., González, J.M., 2014. Master recyclers: features and functions of bacteria associated with phytoplankton blooms. Nat. Rev. Microbiol. 12, 686–698. https://doi.org/10.1038/nrmicro3326.

Callahan, B.J., McMurdie, P.J., Rosen, M.J., Han, A.W., Johnson, A.J.A., Holmes, S.P., 2016. DADA2: high-resolution sample inference from Illumina amplicon data. Nat. Methods 13, 581–583. https://doi.org/10.1038/nmeth.3869.

Conway, J.R., Lex, A., Gehlenborg, N., 2017. UpSetR: an R package for the visualization of intersecting sets and their properties. Bioinformatics 33, 2938–2940. https://doi.org/10.1093/bioinformatics/btx364.

Dahl, E., Bagøien, E., Edvardsen, B., Stenseth, N.C., 2005. The dynamics of Chrysochromulina species in the Skagerrak in relation to environmental conditions. J. Sea Res. 54, 15–24. https://doi.org/10.1016/j.seares.2005.02.004.

Dahl, E., Lindahl, O., Paasche, E., Throndsen, J., 1989. The Chrysochromulina polylepis Bloom in Scandinavian Waters During Spring 1988. In: Cosper, E.M., Bricelj, V.M., Carpenter, E.J. (Eds.), Novel Phytoplankton Blooms. Springer Berlin Heidelberg, Berlin, Heidelberg, pp. 383–405. https://doi.org/10.1007/978-3-642-75280-3_23.

Edvardsen, B., Egge, E.S., Vaulot, D., 2016. Diversity and Distribution of Haptophytes Revealed by Environmental Sequencing and Metabarcoding – A Review. Perspectives in Phycology in press. https://doi.org/10.1127/pip/2016/0052.

Edvardsen, B., Eikrem, W., Throndsen, J., Sáez, A.G., Probert, I., Medlin, L.K., 2011. Ribosomal DNA phylogenies and a morphological revision provide the basis for a revised taxonomy of the Prymnesiales (Haptophyta). Eur. J. Phycol. 46, 202–228. https://doi.org/10.1080/09670262.2011.594095.

Edvardsen, B., Paasche, E., 1998. Bloom dynamics and physiology of Prymnesium and Chrysochromulina. Physiological Ecology of Harmful Algal Blooms. NATO ASI SERIES G ECOLOGICAL SCIENCES. 193–208.

Edvardsen, B., Paasche, E., 1992. Two motile stages of Chrysochromulina polylepis (Prymnesiophyceae): morfology, growth and toxicity. J. Phycol. 28, 12.

Egge, E.S., Eikrem, W., Edvardsen, B., 2015a. Deep-branching Novel Lineages and High Diversity of Haptophytes in the Skagerrak (Norway) Uncovered by 454 Pyrosequencing. J. Eukaryot. Microbiol. 62, 121–140. https://doi.org/10.1111/jeu.12157.

Egge, E.S., Johannessen, T.V., Andersen, T., Eikrem, W., Bittner, L., Larsen, A., Sandaa, R., Edvardsen, B., 2015b. Seasonal diversity and dynamics of haptophytes in the S kagerrak, N orway, explored by high-throughput sequencing. Mol. Ecol. 24, 3026–3042. https://doi.org/10.1111/mec.13160.

Eikrem, W., Throndsen, J., 1998. Morphology and some ultrastructural details of Chrysochromulina leadbeateri Estep et al. (Prymnesiophyceae, Haptophyta) from Northern Norway. Phycologia 37, 292–299.

Eppley, R.W., Holmes, R.W., Paasche, E., 1967. Periodicity in cell division and physiological behavior of Ditylum brightwellii, a marine planktonic diatom, during growth in light-dark cycles. Archiv. Mikrobiol. 56, 305–323. https://doi.org/10.1007/BF00425206.

Estep, K., Davis, P.G., Hargraves, P.E., Sieburth, J., 1984. Chloroplast containing microflagellates in natural populations of north Atlantic nanoplankton, their identification and distribution; including a description of five new species of Chrysochromulina (Prymnesiophyceae). Protistologica (Paris. 1965) 20, 613–634.

Gasol, J.M., Morán, X.A.G., 2015. Flow cytometric determination of microbial abundances and its use to obtain indices of community structure and relative activity. In: McGenity, T.J., Timmis, K.N., Nogales, B. (Eds.), Hydrocarbon and Lipid Microbiology Protocols, Springer Protocols Handbooks. Springer Berlin Heidelberg, Berlin, Heidelberg, pp. 159–187. https://doi.org/10.1007/8623_2015_139.

Gjøsæter, J., Lekve, K., Stenseth, N., Leinaas, H., Christie, H., Dahl, E., Danielssen, D., Edvardsen, B., Olsgard, F., Oug, E., Paasche, E., 2000. A long-term perspective on the Chrysochromulina bloom on the Norwegian Skagerrak coast 1988: a catastrophe or

an innocent incident? Mar. Ecol. Prog. Ser. 207, 201–218. https://doi.org/10.3354/meps207201.

Godhe, A., Sjöqvist, C., Sildever, S., Sefbom, J., Harðardóttir, S., Bertos-Fortis, M., Bunse, C., Gross, S., Johansson, E., Jonsson, P.R., Khandan, S., Legrand, C., Lips, I., Lundholm, N., Rengefors, K.E., Sassenhagen, I., Suikkanen, S., Sundqvist, L., Kremp, A., 2016. Physical barriers and environmental gradients cause spatial and temporal genetic differentiation of an extensive algal bloom. J. Biogeogr. 43, 1130–1142. https://doi.org/10.1111/jbi.12722.

Gran-Stadniczeñko, S., Šupraha, L., Egge, E.D., Edvardsen, B., 2017a. Haptophyte diversity and vertical distribution explored by 18S and 28S Ribosomal RNA Gene Metabarcoding and scanning electron microscopy. J. Eukaryotic Microbiol. 64, 514–532. https://doi.org/10.1111/jeu.12388.

Gran-Stadniczeñko, S., Šupraha, L., Egge, E.D., Edvardsen, B., 2017b. Haptophyte diversity and vertical distribution explored by 18S and 28S Ribosomal RNA gene metabarcoding and scanning electron microscopy. J. Eukaryot. Microbiol. 64, 514–532. https://doi.org/10.1111/jeu.12388.

Guillou, L., Bachar, D., Audic, S., Bass, D., Berney, C., Bittner, L., Boutte, C., Burgaud, G., de Vargas, C., Decelle, J., del Campo, J., Dolan, J.R., Dunthorn, M., Edvardsen, B., Holzmann, M., Kooistra, W.H., Lara, E., Le Bescot, N., Logares, R., Mahé, F., Massana, R., Montresor, M., Morard, R., Not, F., Pawlowski, J., Probert, I., Sauvadet, A.L., Siano, R., Stoeck, T., Vaulot, D., Zimmermann, P., Christen, R., 2013. The Protist Ribosomal Reference database (PR2): a catalog of unicellular eukaryote small sub-unit rRNA sequences with curated taxonomy. Nucl. Acids Res 41, D597–D604. https://doi.org/10.1093/nar/gks1160.

Guiry, M., Guiry, G., 2021. AlgaeBase. World-Wide Electronic Publication. National university of Ireland, Galway. http://www.algaebase.org/.

Hallegraeff, G., Enevoldsen, H., Zingone, A., 2021. Global harmful algal bloom status reporting. Harmful. Algae 102, 101992. https://doi.org/10.1016/j.hal.2021.101992.

Hegseth, E., Eilertsen, H., 1991. The *Chrysochromulina leadbeateri* Bloom in Troms May/June 1991. Development and Causes. Fisken og havet, p. 1991.

Johannessen, T., Larsen, A., Bratbak, G., Pagarete, A., Edvardsen, B., Egge, E., Sandaa, R.-.A., 2017. Seasonal dynamics of haptophytes and dsDNA algal viruses suggest complex virus-host relationship. Viruses 9, 84. https://doi.org/10.3390/v9040084.

John, Uwe, Wisotzki, Andreas, 2019. Physical oceanography during HEINCKE cruise HE533. https://doi.org/10.1594/PANGAEA.903511.

Johnsen, T.M., Eikrem, W., Olseng, C.D., Tollefsen, K.E., Bjerknes, V., 2010. Prymnesium parvum : the Norwegian Experience 1: p rymnesium parvum : t he Norwegian E xperience. JAWRA J. Am. Water Resour. Assoc. 46, 6–13. https://doi.org/10.1111/j.1752-1688.2009.00386.x.

Jones, H., Leadbeater, B., Green, J., 1994. Mixotrophy in haptophytes. System. Assoc. Spec. 51, 247. –247.

Karlson, B., Andersen, P., Arneborg, L., Cembella, A., Eikrem, W., John, U., West, J.J., Klemm, K., Kobos, J., Lehtinen, S., Lundholm, N., Mazur-Marzec, H., Naustvoll, L., Poelman, M., Provoost, P., De Rijcke, M., Suikkanen, S., 2021. Harmful algal blooms and their effects in coastal seas of Northern Europe. Harmful. Algae 102, 101989. https://doi.org/10.1016/j.hal.2021.101989.

Kong, L.-.F., He, Y.-.B., Xie, Z.-.X., Luo, X., Zhang, H., Yi, S.-.H., Lin, Z.-.L., Zhang, S.-.F., Yan, K.-.Q., Xu, H.-.K., Jin, T., Lin, L., Qin, W., Chen, F., Liu, S.-.Q., Wang, D.-.Z., 2021. Illuminating key microbial players and metabolic processes involved in the remineralization of particulate organic carbon in the Ocean's twilight zone by metaproteomics. Appl. Environ. Microbiol. 87 https://doi.org/10.1128/AEM.00986-21 e00986-21.

Lackey, J.B., 1939. Notes on plankton flagellates from the Scioto River. Lloydia 2, 128–141.

Legendre, P., Gallagher, E., 2001. Ecologically meaningful transformations for ordination of species data. Oecologia 129, 271–280. https://doi.org/10.1007/s004420100716.

Lekve, K., Bagøien, E., Dahl, E., Edvardsen, B., Skogen, M.D., Stenseth, N.C., 2006. Environmental forcing as a main determinant of bloom dynamics of the Chrysochromulina algae. Proc. Biol. Sci. 273, 3047–3055. https://doi.org/10.1098/rspb.2006.3656.

Mardones, J.I., Fuenzalida, G., Zenteno, K., Alves-de-Souza, C., Astuya, A., Dorantes-Aranda, J.J., 2019. Salinity-Growth Response and Ichthyotoxic Potency of the Chilean Pseudochattonella verruculosa. Front. Mar. Sci. 6, 24. https://doi.org/10.3389/fmars.2019.00024.

Marthinussen, Nystøyl, Storhaug, Valle, Gaarder, 2020. Økonomiske Og Samfunnsmessige Konsekvenser Av Algeoppblomstringen i Havbruksnæringen i Nord-Norge. KONTALI (in Norwegian).

Martin, M., 2011. Cutadapt removes adapter sequences from high-throughput sequencing reads. EMBnet J 17, 10. https://doi.org/10.14806/ej.17.1.200.

Nielsen, T.G., Kiørboe, T., Bjørnsen, P.K., 1990. Effects of a *Chrysochromulina polylepis* subsurface bloom on the planktonic community. Mar. Ecol. Prog. Ser. 21–35.

Oksanen, J., Blanchet, F.G., Kindt, R., Legendre, P., O'Hara, R.B., Simpson, G.L., Solymos, P., Stevens, M.H.H., Wagner, H., 2020. Vegan: Community Ecology Package. R Package Version 1.17-2. R Foundation for Statistical Computing, Vienna.

Parada, A.E., Needham, D.M., Fuhrman, J.A., 2016. Every base matters: assessing small subunit rRNA primers for marine microbiomes with mock communities, time series and global field samples: primers for marine microbiome studies. Environ. Microbiol. 18, 1403–1414. https://doi.org/10.1111/1462-2920.13023.

Piredda, R., Tomasino, M.P., D'Erchia, A.M., Manzari, C., Pesole, G., Montresor, M., Kooistra, W.H.C.F., Sarno, D., Zingone, A., 2017. Diversity and temporal patterns of planktonic protist assemblages at a mediterranean long term ecological research site. FEMS Microbiol. Ecol. 93, 1–14. https://doi.org/10.1093/femsec/fiw200.

R Core Team, 2020. R: A language and Environment for Statistical Computing. R Foundation for Statistical Computing, Vienna, Austria.

Rey, F., 1991. Oppblomstringen av *Chrysochromulina leadbeateri* i Vestfjorden, mai-juni 1991: rapport fra et faglig arbeidsseminar.

Rohardt, G., 2019. CTD Processing Report of RV Heincke HE533.

Ruggiero, M.V., D'Alelio, D., Ferrante, M.I., Santoro, M., Vitale, L., Procaccini, G., Montresor, M., 2017. Clonal expansion behind a marine diatom bloom. ISME J 12, 463–472. https://doi.org/10.1038/ismej.2017.181.

Samdal, I.A., Edvardsen, B., 2020. Massive salmon mortalities during a *Chrysochromulina leadbeateri* bloom in Northern Norway. Harmful Algal News 64, 4–5.

Skjoldal, H.R., Dundas, I., 1991. The *Chrysochromulina Polylepis* Bloom in the Skagerrak and the Kattegat in May-June 1988: Environmental Conditions, Possible Causes, and Effects: Report of the ICES Workshop on the *Chrysochromulina Polylepis* Bloom in the Skagerrak and Kattegat in May-June 1988, Bergen, 28 February-2 March 1989. International Council for the Exploration of the Sea.

Stamatakis, A., 2014. RAxML version 8: a tool for phylogenetic analysis and post-analysis of large phylogenies. Bioinformatics 30, 1312–1313. https://doi.org/10.1093/bioinformatics/btu033.

Teeling, H., Fuchs, B.M., Becher, D., Klockow, C., Gardebrecht, A., Bennke, C.M., Kassabgy, M., Huang, S., Mann, A.J., Waldmann, J., 2012. Substrate-controlled succession of marine bacterioplankton populations induced by a phytoplankton bloom. Science 336, 608–611.

Teeling, H., Fuchs, B.M., Bennke, C.M., Krueger, K., Chafee, M., Kappelmann, L., Reintjes, G., Waldmann, J., Quast, C., Gloeckner, F.O., 2016. Recurring patterns in bacterioplankton dynamics during coastal spring algae blooms. Elife 5, e11888.

Thomsen, H.A., Buck, K.R., Chavez, F.P., C.L.B.S., 1994. Haptophytes as components of marine phytoplankton (Ed.). The Haptophyte Algae. Clarendon Press, Oxford, p. 187.

Throndsen, J., Hasle, G.R., Tangen, K., 2007. Phytoplankton of Norwegian Coastal Waters. Almater.

Wells, M.L., Trainer, V.L., Smayda, T.J., Karlson, B.S.O., Trick, C.G., Kudela, R.M., Ishikawa, A., Bernard, S., Wulff, A., Anderson, D.M., Cochlan, W.P., 2015. Harmful algal blooms and climate change: learning from the past and present to forecast the future. Harmful Algae 49, 68–93. https://doi.org/10.1016/j.hal.2015.07.009.

Wolf, K.K.E., Hoppe, C.J.M., Leese, F., Weiss, M., Rost, B., Neuhaus, S., Gross, T., Kühne, N., John, U., 2021. Revealing environmentally driven population dynamics of an Arctic diatom using a novel microsatellite PoolSeq barcoding approach. Environ Microbiol 23, 3809–3824. https://doi.org/10.1111/1462-2920.15424.

Zhongming, Z., Linong, L., Wangqiang, Z., Wei, L., others, 2021. AR6 climate change 2021: the physical science basis.